



ISSN: 0976-3031

Available Online at <http://www.recentscientific.com>

CODEN: IJRSFP (USA)

International Journal of Recent Scientific Research

Vol. 14, Issue, 06 (C), pp. 3488-3492, June, 2023

**International Journal of
Recent Scientific
Research**

DOI: 10.24327/IJRSR

Research Article

A NOVEL ANFIS CONTROLLER BASED WATER PUMPING SYSTEM WITH GRID CONNECTED RES

Charishma T¹, R R Prasad² and Durga Sukumar G³

¹Department of PEED, Vignan Institute of Science and Technology, Near Ramoji Film City, Deshmukhi, Yadadri Bhuvanagiri (Dist), Telangana

^{2,3}Department of Electrical & Electronics Engineering, Vignan Institute of Science and Technology, Near Ramoji Film City, Deshmukhi, Yadadri Bhuvanagiri(Dist), Telangana

DOI: <http://dx.doi.org/10.24327/ijrsr.2023.1406.0709>

ARTICLE INFO

Article History:

Received 12th March, 2023

Received in revised form 23rd

April, 2023

Accepted 7th May, 2023

Published online 28th June, 2023

Keywords:

Renewable Energy Source

ABSTRACT

Bidirectional power flow here between renewable energy source (RES) and also the load is implemented in this work. Renewable energy (RES) is generated using solar photovoltaic (PV) cells and a BLDC motor load is linked to the water pump via a single stage bi-directional converter & voltage source inverter (VSI) in the system to power the water pump. Fusing in the solar generating framework allows the solar power generation system to extract maximum power while reducing grid losses and enabling consumers to run their motors and loads at their maximum efficiency all day long. Adaptive neuro fuzzy interface system (ANFIS) in the Photovoltaic reduces switching costs, total harmonic distortion of the grid, etc. while preserving the system's power factor, quality of power, and system stability.

Copyright© The author(s) 2023. This is an open-access article distributed under the terms of the Creative Commons Attribution License, which permits unrestricted use, distribution and reproduction in any medium, provided the original work is properly cited.

INTRODUCTION

It's a no-brainer for customers to switch to renewable energy as carbon emissions continue to rise and fossil resources become more scarce. Conventional energy sources are being replaced by solar photovoltaic (PV) output. As a result of this, PV water pumping has attracted a lot of attention during the past several decades. The water was first pumped by DC motors, then by an AC motor. Many studies have been carried out and on electric drive drives for PV-fed pump systems to increase performance and efficiency at a lower cost. Permanent magnetic DC (BLDC) motors have been more popular in recent years because of their high efficiency, high power density, no upkeep, extended service life, minimal electromagnetic interference (EMI) concerns, and compact size. Incorporating this motor lowers the cost & size of PV panels, while also improving performance and eliminating the need for maintenance.

Existing BLDC motor-driven water pumps fueled by a PV array that are not connected to the grid depend solely on PV solar energy. Solar PV generating reveals its fundamental shortcomings, resulting in an unstable water pumping system,

due to its intermittent nature. Because of extreme climatic conditions and underutilization of the pump, water pumping has been seriously disrupted. In addition, a lack of sunshine (at night) causes the water pumping mechanism to stop down. In order to have a dependable PV pumping system, several issues must be addressed. There have been a few efforts to use a battery to store energy in this context, but not with BLDC motor drives. Batteries are charged and discharged in tandem with an unidirectional control, ensuring a constant supply of water even when the sun isn't shining. Energy storage system in PV crop irrigation not only raises the total cost and maintenance, but also affects the service life of this pumping system. A typical lead acid battery has a functional life of only two to three years.

As previously indicated, the disadvantages of battery storage have shifted focus to an other technical option that may be more suitable for a dependable water pumping system that relies on solar photovoltaic power in all respects. A PV generating unit erected for water pumping may be connected to the utility grid using these newly recognized technologies. Regardless of operational circumstances, day or night, the

*Corresponding author: **Charishma T**

Department of PEED, Vignan Institute of Science and Technology, Near Ramoji Film City, Deshmukhi, Yadadri Bhuvanagiri (Dist), Telangana

primary goal is to provide continual water pumping at its maximum capacity. Water pumping systems using solar electricity have been described in which an allocation mechanism selects whether to use the PV array or the utility grid (when PV array is insufficient to power the pump). The shared DC bus of the PV array and the grid-connected inverter is linked to a water pump and pump controller. Maintenance and production costs are decreased as a result of the absence of battery storage. This regulation allows just one-way power flow, which means that any surplus or unutilized electricity from the PV array is just not returned to a utility grid. As a result, the PV system is not completely used, and a client is still required to pay for power.

Second, the utility grid is powered by a utility grid inverter, and then the water pump is fed by the utility grid inverter via a pump inverter [13]. However, it looks to be a system that is exclusively powered by the utility grid. According to [15], a voltage regulator and an inverter may be used to charge and discharge a battery, which can then be used to power a water pump. A utility interface is also provided via an option switch on the pump. In order to keep this system affordable, the battery storage is required. In [16-17], a portion of the PV system is used to pump water, while the rest is used to provide electricity to the grid. Because the pumping is solely powered by the solar panels, the system is unreliable. This is a grid-interfacing PV-fed BLDC motor driven pumping stations system with directional power flow regulation, in which the remainder power is obtained from the grid as necessary. When water pumping isn't needed, the new technology wastes solar electricity.

This means that all of the above-mentioned known topologies of a PV-based pumping system have a one-way power flow control. In order to make the most of both the PV installation and the pumping system, a multifunctional system that allows for bidirectional power flow is still being designed. A BLDC diesel engine is used for the first time in this system. If a water pump is not needed, the suggested system will allow for the transfer of electricity from PV arrays to single-phase utility grids, and vice versa, if PV array output is not adequate (or at night) to operate BLDC motor-pump at its maximum capability. Consumers may profit from the selling of their excess power to the utility in this way. In order to execute a bi-directional power transfer, a simple unit vector template (UVT) creation is used.

Circuit Description

A BLDC motor drives a water pump in the proposed pumping system. A buck converter and VSI provide power to a BLDC motor pump from a PV array. PV array MPPT is performed by the boost converter using InC algorithm, whereas BLDC motor electronic commutation occurs through the VSI [5, 26]. To perform an electrical commutation, a built-in encoder creates three Hall-effect signals. A single-phase utility grid provides power to the VSI DC bus. Through with a DC bus capacitor, a voltage converter (VSC) permits bidirectional power transmission. When hydro power is not necessary, the Pv system feeds the grid. Otherwise, it is a desired aim. Power may flow between both the grids and VSC through an interface inductor, which also serves to minimize harmonics entering the supply. In order to reduce harmonics on the supply voltage, an RC ripple filtering is supplied. Appendices provide a comprehensive mathematical model of the whole system.

Speed Control of Blcdmotor

In the last section, we examined how the suggested BLDC motor drive would remove the phase shift sensors. Regardless of the weather, the BLDC motor-pump should be able to run at its specified speed. Maintaining the VSI's DC bus voltage at its rated DC voltage allows for this. By controlling the Bus voltage and thus the operating speed, a b) non power flow control is able to supply the entire amount of power necessary to pump the water at maximum capacity. Under adverse weather circumstances, the BLDC motor's rated DC voltage is not maintained, and the speed is controlled by a changeable DC bus voltage.

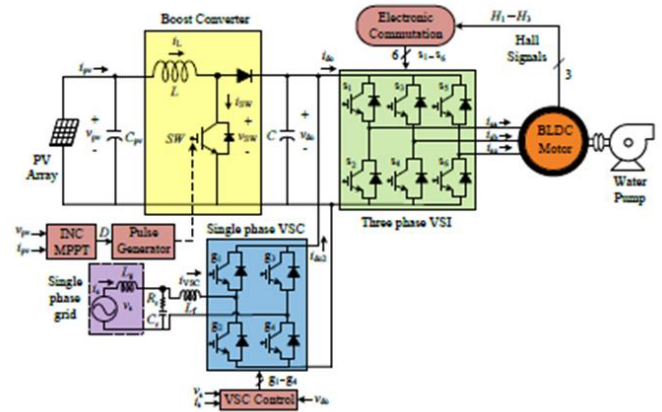


Figure 1 Schematic of the grid interactive PV array based water pumping system using BLDC motor drive

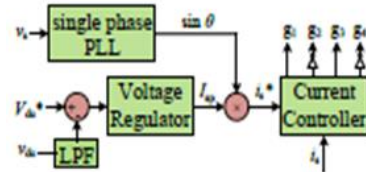


Figure 2 UVT based bi-directional power flowcontrol of VSC

BI-Directional Power Flow CONTROL

System reliability and maximum use of resources are achieved by a grid-interactive PV generation, which is capable of producing dependable water pumping systems. Figure 2 shows a bi-directional voltage regulation based on a Space vector modulation generation [20, 27-28]. Because it doesn't need a sophisticated mathematical model or procedure, this is the simplest approach. The grid power voltage and current are synchronized using a single stage PLL (Phase Locked Loop). Supply voltage, sin sine wave, is generated at the fundamental frequency. It is also possible to regulate the DC bus voltage (vdc) to extract the important element of supply current, Isp. A PI controller is used to regulate the voltage of the system. First-order low pass filters are used to reduce the amplitude of the vdc signal. It is then tested against the predetermined value, Vdc*. Isp and sin are multiplied to get a basic supply current component, is*. Gating pulses for the VSC are generated by comparing the measured supply current, is, to is* and calculating an error.

The voltage regulator creates a positive Isp when it is necessary to draw electricity from the utility. As a result, the grid receives an in-phase supply current. Because of this, an out-of-phase accessibility of resources is created so when utility is supplied by a PV array. When the flow of power is reversed, the desired direction of flow may be achieved. Total harmonic distortion (THD) and voltage level (PF) are also enhanced as a result of

the applied control approach. The Output dc voltage is controlled if the grid is unavailable. It's still possible to run the water pump on its own, though, thanks to the PV array's ability to adapt to changing weather conditions. Appendices provide a full examination of the proposed bidirectional power regulation.

System Design

The PV array, power converter, single-phase grid, single-phase VSC, three-phase VSI, and BLDC motor, which are all part of the arrangement depicted in Fig. 1, are all carefully chosen to provide the best possible performance. This section explains the design methods used for these components.

Design of PV Array

A 1.3 kW BLDC motor-pump requires a 1.5 kWp-PV array. The converters and motor-pump power losses are taken into consideration. To estimate the parameters, we use the usual test setting (1000 W/m², 25°C, AM 1.5). [29] In order to create a PV array with the needed capacity, the Solar panel with only an MPP voltage of 28.5 V as well as an MPP current of 7.5 A is selected. A PV array's output voltage is first determined by taking into account the BLDC motor's DC voltage rating, or the DC bus voltage, at MPP. The parameter $V_{mpp} = v_{pv} = 200$ V is chosen and the following values are computed as a result

Design of Boost Converter

The design of a boost converter consists of an estimation of input inductor, L . It is selected in a manner to operate the converter in CCM, irrespective of the weather condition. The duty ratio, D_1 is estimated as [30],

$$D_1 = \frac{V_{dc} - v_{pv}}{V_{dc}} = \frac{270 - 200}{270} = 0.25 \quad (4)$$

Where $V_{dc} = 270$ V is the DC bus voltage of the VSI. The inductor, L is estimated as,

$$L = \frac{D_1 v_{pv}}{f_{sw} \Delta I_L} = \frac{0.25 \times 200}{10000 \times (7.5 \times 0.2)} = 3.3 \text{ mH} \quad (5)$$

Where f_{sw} is the switching frequency of boost converter; ΔI_L is ripple in the current through L , $\Delta I_L (= I_{mpp})$.

Design of Three Phase VSI

A three phase VSI is used to feed the BLDC motor. Its design consists of an estimation of voltage, current and VA ratings. As the DC bus voltage is 270 V, the required voltage rating of an IGBT switch is calculated as,

$$V_{VSI} = V_{dc} \times 1.4 = 270 \times 1.4 = 378 \approx 400 \text{ V} \quad (6)$$

A voltage safety factor of 1.4 is selected to accommodate the switching transients. Similarly, the required current rating of an IGBT switch is calculated as,

$$I_{VSI} = I_{dc} \times 1.3 = (1500/270) \times 1.3 = 7.23 \approx 7.5 \text{ A} \quad (7)$$

Where 1.3 is a current safety factor.

Finally, the required VA rating of VSI is estimated as,

$$VA_{VSI} = V_{VSI} \times I_{VSI} = 400 \times 7.5 = 3 \text{ kVA} \quad (8)$$

Design of Single Phase VSC

A single-phase VSC is used to control a bidirectional power flow. In a single-phase VSC, the blocking voltage of switching devices is equal to the DC link voltage. As the DC link voltage is 270 V, the switches have to block this voltage. A safety factor of 1.4 is selected to accommodate the voltage transients due to a high frequency switching. Therefore, the voltage rating of the IGBT devices are estimated as,

$$V_{VSC} = V_{dc} \times 1.4 = 270 \times 1.4 = 378 \approx 400 \text{ V} \quad (9)$$

The VSC has a maximum current drawn from the grid or to be fed to the grid. The said current is estimated as,

$$I_{i,max} = \sqrt{2} \frac{P_{mpp}}{V_s} = \sqrt{2} \frac{1500}{180} = 11.78 \text{ A} \quad (10)$$

Where $V_s = 180$ V is rms value of the utility grid voltage. Thus, the maximum current rating of IGBT devices is 11.78 A. Considering a safety factor of 1.3, the current rating is estimated as,

$$I_{VSC} = I_{i,max} \times 1.3 = 11.78 \times 1.3 = 15.3 \approx 15 \text{ A} \quad (11)$$

Finally, the required VA rating of VSC is estimated as,

$$VA_{VSC} = V_{VSC} \times I_{VSC} = 400 \times 15 = 6 \text{ kVA} \quad (12)$$

Design of Common DC Link Capacitor

The DC link capacitor, C is common to the boost converter, three phase VSI and single phase VSC. It is tuned for the second harmonic component of single phase grid voltage, which is appeared on the DC bus of a single phase VSC. Thus, the capacitor, C is estimated as [31],

$$C = \frac{I_{dc}}{2\omega_L \Delta V_{dc}} = \frac{1500/270}{2 \times (2\pi \times 50) \times (270 \times 0.008)} = 4700 \text{ } \mu\text{F} \quad (13)$$

Where I_{dc} is an average current flowing through the DC bus, ω_L is the line frequency in rad/s, and ΔV_{dc} is ripple in the DC bus voltage.

Design of Interfacing Inductor

The selection of an interfacing inductor, L_f depends on the permitted current ripple ΔI_{VSC} . It is estimated as,

$$L_f = \frac{mV_{dc}}{4af_{sw} \Delta I_{VSC}} = \frac{1 \times 270}{4 \times 1.2 \times 10000 \times (1500/180) \times 0.2} = 3.3 \text{ mH} \quad (14)$$

Where modulation index, $m = 1$, over loading factor, $a = 1.2$, switching frequency, $f_{sw} = 10$ kHz, current ripple, $\Delta I_{VSC} = 20\%$ of I_{VSC} .

Design of R-C Ripple Filter

A first order high pass filter is used to suppress the switching harmonics generated by the VSC. A small R-C filter is connected at the utility grid side. This ripple filter is designed such that it offers very high impedance to the fundamental frequency component and low impedance to the switching frequency component. In order to meet this condition, $RrCr \ll T_{sw}$; where R_r , C_r and T_{sw} are respectively the ripple filter resistance, ripple filter capacitance and switching time. Considering $RrCr = T_{sw}/4$, $T_{sw} = 1/10000$ s and $R_r = 5 \text{ } \Omega$, C_r is estimated as [32],

$$C_r = \frac{T_{sw}}{4R_r} = \frac{1}{10000 \times 4 \times 5} = 5 \text{ } \mu\text{F} \quad (15)$$

Thus, a series combination of 5 Ω resistance and 5 μF capacitance is selected as a RC ripple filter.

Extension of project

Improvement of power System Stability Parameters Using Fuzzy

Adaptive Network based Fuzzy Inference System:

In the adaptive network-based fuzzy inference system (ANFIS), the neural network method to solving function approximation issues is represented by a data driven mechanism. Most data-driven approaches for creating ANFIS networks start by clustering samples of the fractional derivative to be approximation in the training data. Classification, rule-based process management, pattern recognition, and other applications of ANFIS networks have proven effective since their debut. The fuzzy model introduced by Takagi, Sugeno, and Kang to define a systematic technique to produce fuzzy sets from an input/output data set is included in this fuzzy inference system.

ANFIS structure

The heuristic under study is considered to have two or more inputs for simplicity's sake. Takagi and Sugeno's fuzzy if-then rules are included in the rule base as follows:

A and B are the fuzzification in the antecedents, and the resultant is $z = f(x,y)$ where $z = f(x,y)$ is a crisp function. A quadratic for the two input variables is usually used. Any other function that may approximate the output in a fuzzy zone can also be used in place of it. While Mamdani [144] fuzzy inference systems are often used, the zero-order Sugeno fuzzy model [144] might be seen as an exception, because each rule consequence is described by a fuzzy singleton. A first-order Sugeno fuzzy model is generated if $f(x,y)$ is a first-order polynomial. The two rules for a first-order two-rule Sugeno fuzzy system are:

$$f1 = p1x + q1y + r1 \text{ if } x \text{ is } A1 \text{ while } y \text{ is } B1.$$

This is the second rule of the game: If you have x in the A2 position and you've got it in the B2 position, then you'll get the following formula:

Here, Takagi and Sugeno [143] designed a type-3 fuzzy inference system. A constant term is added to each rule's output to make it a linear mix of the input variables. Weighted average of each rule's output produces final result. Fig. 4.5 depicts the ANFIS structure that would be equal to this.

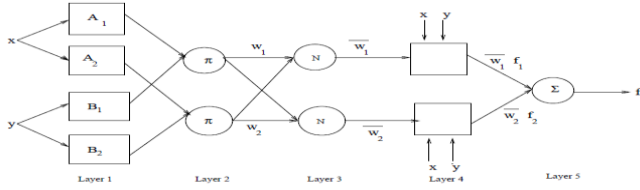


Figure 1 Type-3 ANFIS Structure

The individual layers of this ANFIS structure are described below :

Layer 1: Every node i in this layer is adaptive with a node function

$$O_i^1 = \mu_{A_i}(x) \tag{4.1.1}$$

Where, x is the input to node i , A_i is the linguistic variable associated with this node function and μ_{A_i} is the membership function of A_i . Usually $\mu_{A_i}(x)$ is chosen as

$$\mu_{A_i}(x) = \frac{1}{1 + \left[\frac{(x - c_i)}{a_i} \right]^{2b_i}} \tag{4.1.2}$$

Or

$$\mu_{A_i}(x) = \exp \left\{ - \left(\frac{x - c_i}{a_i} \right)^2 \right\} \tag{4.1.3}$$

Where x is the input and $\{a_i, b_i, c_i\}$ is the premise parameter set.

Layer 2: Each node in this layer is a fixed node which calculates the firing strength w_i of a rule.

The output of each node is the product of all the incoming signals to it and is given by,

$$O_i^2 = w_i = \mu_{A_i}(x) \times \mu_{B_i}(y), \quad i = 1, 2 \tag{4.1.4}$$

Layer 3: Every node in this layer is a fixed node. Each i th node calculates the ratio of the i th rule's firing strength to the sum of firing strengths of all the rules. The output from the i th node is the normalized firing strength given by,

$$O_i^3 = \bar{w}_i = \frac{w_i}{w_1 + w_2}, \quad i = 1, 2 \tag{4.1.5}$$

Layer 4: Every node in this layer is an adaptive node with a node function given by

$$O_i^4 = \bar{w}_i f_i = \bar{w}_i (p_i x + q_i y + r_i), \quad i = 1, 2 \tag{4.1.6}$$

Where \bar{w}_i is the output of Layer 3 and $\{p_i, q_i, r_i\}$ is the consequent parameter set.

Layer 5: This layer comprises of only one fixed node that calculates the overall output as the

Summation of all incoming signals, i.e.

$$O_i^5 = \text{overall output} = \sum_1 \bar{w}_i f_i = \frac{\sum_1 w_i f_i}{\sum_1 w_i} \tag{4.1.7}$$

SIMULATION RESULTS

The MATLAB/Simulation platform is used to simulate different operational circumstances for the proposed system. Starting, static, and steady-state operations of the created system and its control are all tested. Single-phase 180 V, 50 Hz utility grid and a 1.5-kWp PV array (under typical test circumstances) provide the necessary power for a 4-pole 3000-r/min pump at 270 V (dc). Additional information on the system is provided in the appendices. For example, the water pump may be powered by a PV array, the grid, or a combination of the two. In order to test out the suggested system, we take into account all of these conceivable operational circumstances

Starting and Steady-State Performance

Studies on motor pump performance are primarily concerned with demonstrating the BLDC motor's ability to start softly and maintain a steady state under a variety of operating situations.

When only PV array feeds BLDC motor pump

As indicated in Fig. 2, the PV array is operating at its MPP under the radiation intensity of 1000 W/m² as shown in Fig. 3. For this reason, as can be seen in Fig. 4.2.1, we run the Dc motors pump at its rated speed of 3000 revolutions per minute (rpm) (b). The PV array provides enough electricity to operate the pump at full capacity, so there is no need for grid power. EMF, stator current, speed, electromagnetic torque, and load torque are all referenced by the different indices. The motor pump's steady-state performance and gentle starting are both shown in these data.

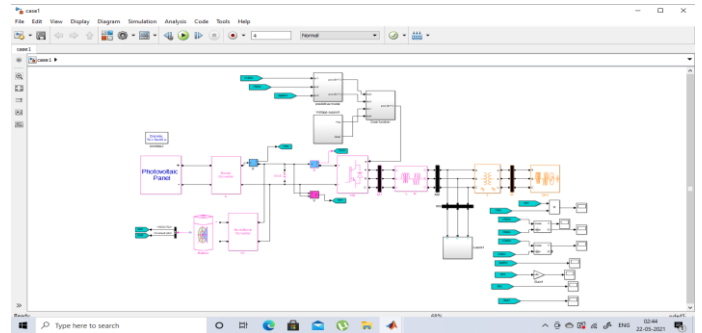


Figure 1 Simulation Circuit diagram when only PV array feeds BLDC motor pump

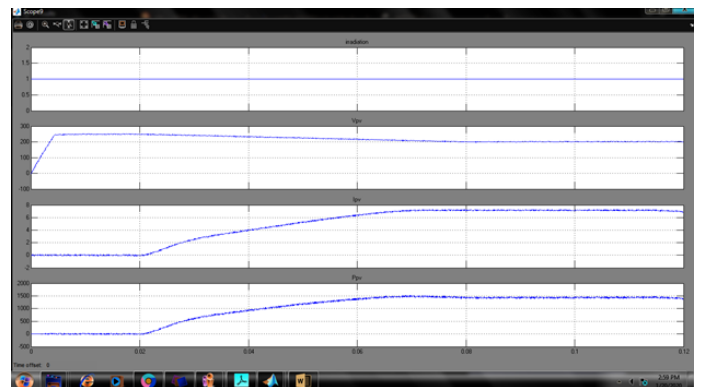


Figure 2 Steady state and starting performance of PVarray, when only PV array feeds BLDC motor-pump

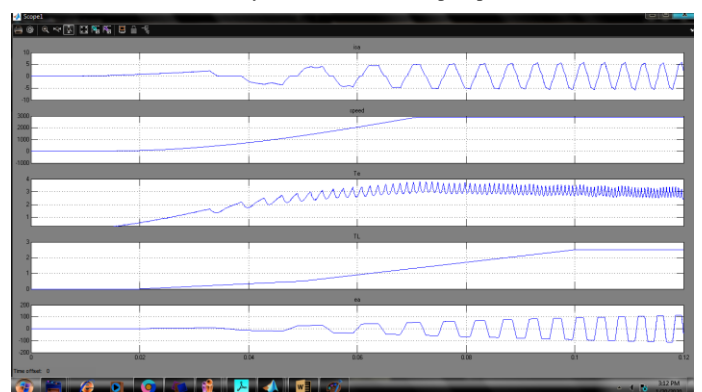


Figure 3 Steady state and starting performance of (b) BLDCmotor-pump, when only PV array feeds BLDC motor-pump

When only utility grid feeds BLDC motor pump:

When nighttime water pumping is necessary, this operational state develops. A sinusoidal source current of 8.3 A (rms) is used and the voltage output is maintained at 270 V as shown in Fig. 5. Figure 4 shows that the motor is able to draw enough power from the utility to operate at full capacity (b). In this situation, the pumping mechanism is fully used.

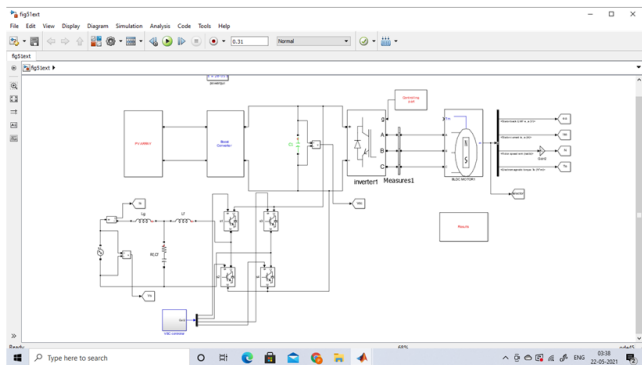


Figure 4 Simulation Circuit diagram when only utility grid feeds BLDC Motor pump

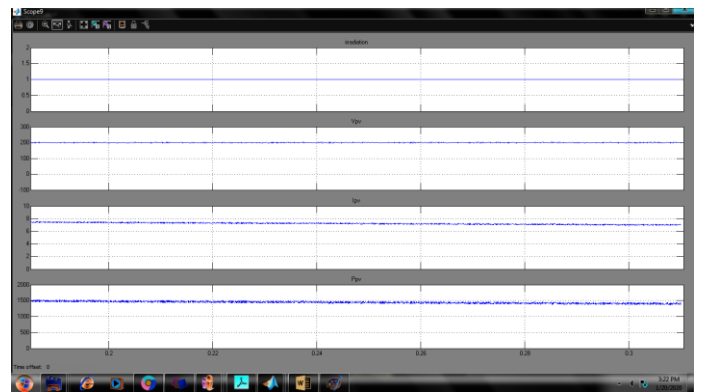


Figure 8 Study state response of PV-Array, when water pumping is not required

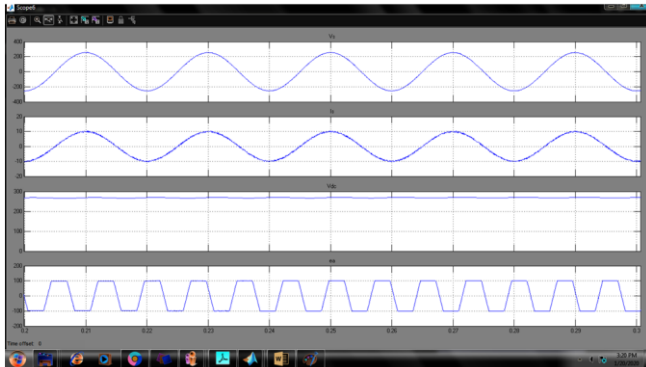


Figure 5 Starting and steady state performance of utility grid, when only utility grid feeds water pump

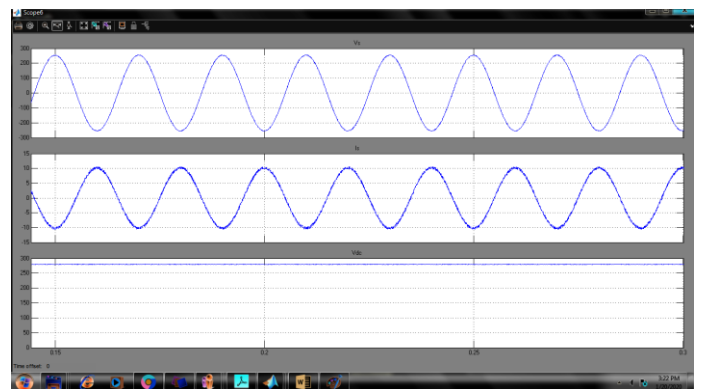


Figure 9 Study state response of Utility Grid, when water pumping is not required

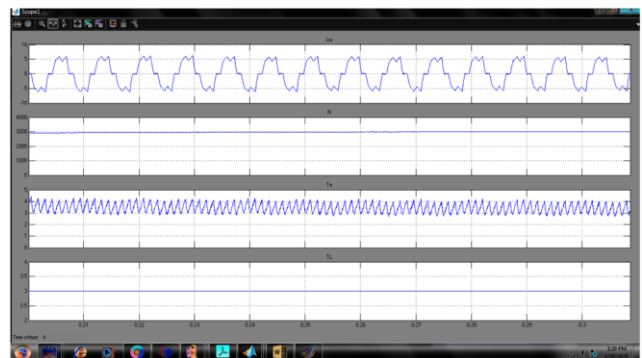


Figure 6 Starting and steady state performance of (b) BLDC motor-pump, when only utility grid feeds water pump

When water pumping is not required

Power from the PV array is supplied into the utility grid in this situation, and no pumping is required. PV array MPP operating at 1000 W/m² is shown in Fig. 7. Out-of-phase supply current in Fig. 8 implies the utility is supplied by a PV array as well as the output current is reversed while retaining 270 V dc. 5

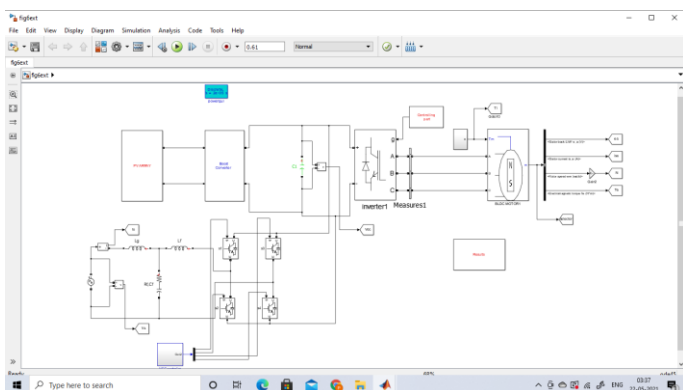


Figure 7 Simulation Circuit Diagram when water pumping is not required

CONCLUSION

This research proposes an ANFIS-based single-phase grid-interactive PV array-based water pumping system with a BLDC motor drive. VSC's bi-directional power flow regulation has allowed for complete use of resources for water pumping at max capability regardless of the weather. In order to manage the flow of electricity, a basic UVT generating approach has been used. The IEEE-519 standard's requirements for power quality have all been satisfied. BLDC motor-pump speed control has been accomplished without the need of current sensors. The total efficiency of the system has been improved by a fundamental switching frequency of VSI, which has reduced switching losses. Too far, the water pumping system suggested has shown itself to be both dependable and profitable for the utility company when groundwater is not necessary.

References

1. M.T.A.Khan, G.Norris, R.Chattopadhyay, I.Hussain and S.Bhattacharya, "Autoinspection and Permitting With a PV Utility Interface (UPI) for Residential Plug-and-Play Solar Photovoltaic Unit," IEEE Trans. Ind. Appl., vol. 53, no. 2, pp.1337-1346, March-April 2017.
2. M.Montorfano, D.Sbarbaro and L.Moran, "Economic and Technical Evaluation of Solar-Assisted Water Pump Stations for MINING Applications: A Case of Study," IEEE Trans. Ind. Appl., vol. 52, no. 5, pp.4454-4459, Sept.-Oct.2016.